



Performance Analysis of a Direct Absorption Solar Collector using Different Nanofluids: Effect of Physical Parameters

Salma Parvin^{*a}, Abrar Islam^b, and Afroza Nahar^c

^a Department of Mathematics, Bangladesh University of Engineering and Technology, Dhaka 1000, Bangladesh

^b Department of Chemical and Materials Engineering, University of Alberta, 9211 116 Street NW, Edmonton T6G 1H9, Alberta, Canada

^c Department of Computer Science, American International University – Bangladesh, Dhaka 1229, Bangladesh

ABSTRACT

Nanofluids have been used in direct absorption solar collectors (DASC) to enhance their performance, wherein contribution of entropy generation plays a decisive role. Among other factors, entropy generation is influenced including physical structure of the system and operation conditions. In this article, heat transfer and efficiency of a nanofluid based DASC considering the entropy generation has been performed for various physical alterations and operating conditions. Working nanofluids are chosen to Cu-water nanofluid, Al₂O₃-water nanofluid, TiO₂-water nanofluid and water is chosen as base fluid. Solar irradiation value for the current analysis is considered 225W/m² from the annual average solar irradiance range (215 W/m² in the north-west to 235 W/m² in the south-west per day) in Bangladesh according to UNDP report. Governing equations consisting of Navier–Stokes and energy equations are solved by Penalty finite element method with Galerkins weighted residual approach. Impact of parameters nanoparticle concentration and thickness of flow on isotherms, average output temperature, the average Nusselt number, collector efficiency, average entropy generation and Bejan number are discussed for all considered fluids. Results reveal that DASC system exhibits efficacy in heat transfer using 2% Cu nanoparticles under 225W/m² irradiance, 0.015 kg/s mass flow rate and 0.015 m flow thickness. The outcomes will be supportive in designing DASC to attain improved heat transfer performance considering entropy generation.

© 2021 Published by Bangladesh Mathematical Society

Received: August 18, 2021 **Accepted:** November 11, 2021 **Published Online:** January 07, 2022

Keywords: DASC; nanofluid; solar irradiation heat transfer performance; flow depth; entropy.

AMS Subject Classification 2020: 76M10; 80M10; 80A19

1. Introduction

Energy demand is growing day by day, but fossil fuels are limited. Renewable energy sources, especially solar energy is considered as reliable source with very little ecological impact. The hourly incident solar flux

* Corresponding author: Salma Parvin, *E-mail address:* salpar@math.buet.ac.bd

on the earth's surface is greater than the global annual energy consumption [1]. However, the challenge is to efficiently harvest and convert the solar energy into the useful form. Solar collectors convert the solar energy into heat and flat-plate or evacuated-tube solar collectors are the commonly used devices in this regard. Recently, a new type of collector namely direct absorption solar collector (DASC) [2] have been developed that offer enhanced thermal efficiency.

However, the main drawback with DASC collectors is the poor absorption properties of conventional fluids used in these collectors. To solve this problem, researchers tried the use of nanofluids in DASC because of their improved thermal properties over the conventional fluids [3]. Heat transfer enhancement in solar devices is one of the key issues of energy saving and compact designs. An attempt had been made by Verma and Kundan [4] to experimentally investigate the variation in collector efficiency using nanofluids in a DASC. Parvin et al. [5] investigated the influence of Reynolds number and solid volume fraction of nanofluid in heat transfer through a nanofluid based direct absorption solar collector. Tyagi et al. [6] theoretically investigated the efficiency of a nanofluid-based direct absorption solar collector and compared it to the typical flat plate collector. Otanicar et al. [7] reported on the experimental results on solar collectors based on nanofluids where they demonstrated efficiency improvements of up to 5% in solar thermal collectors by utilizing nanofluids. Mahian et al. [8] made a review of the applications of nanofluids in solar energy. Two-phase (non-homogeneous) nanofluid approach towards the convection heat transfer within a wavy direct absorber solar collector is reported by Alsabery et al. [9].

All thermofluidic processes involve irreversibilities and therefore incur an efficiency loss. In practice, the extent of these irreversibilities can be measured by the entropy generation rate. In designing practical systems, it is desirable to minimize the rate of entropy generation to maximize the available energy. Bejan[10,11] studied on entropy generation minimization in order to minimize the irreversibility associated with convective heat transfer process. Mixed convection and entropy generation of Cu–water nanofluid in a cavity was numerically studied by Khorasanizadeh et al. [12]. They showed the influence of Reynolds number in enhancing heat transfer and minimizing entropy generation. Mohseni-Languri et al. [13] performed experimental study on energy and exergy of a solar thermal air collector. The rate of entropy generation increases as the irreversibility distribution ratio increase. Moreover, for given values of the irreversibility distribution ratio, the entropy generation rate is determined by the heat transfer irreversibility and/or fluid friction irreversibility.

Shahi et al. [14] investigated the entropy generation induced by natural convection heat transfer in a square cavity containing Cu-water nanofluid and a protruding heat source. Results showed that the Nusselt number increased and the entropy generation reduced as the nanoparticle volume fraction was increased. In addition, it was shown that the heat transfer performance could be maximized, and the entropy generation minimized by positioning the heat source on the lower cavity wall. Esmailpour and Abdollahzadeh [15] examined the natural convection heat transfer behavior and entropy generation rate in a Cu-water nanofluid-filled cavity comprising two vertical wavy surfaces with different temperatures and two horizontal flat surfaces with thermal insulation. The results showed that the mean Nusselt number and entropy generation rate both decreased as the volume fraction of nanoparticles increased. It was also shown that the mean Nusselt number and rate of entropy generation both increased with an increasing Grashof number but decreased with an increasing surface amplitude.

Cho et al. [16] investigated the natural convection heat transfer performance and entropy generation rate in a water-based nanofluid-filled cavity bounded by a left wavy-wall with a constant heat flux, a right wavy-wall with a constant low temperature, and flat upper and lower walls with adiabatic conditions. Results showed that the mean Nusselt number increased and the entropy generation rate decreased as the volume fraction of nanoparticles increased. Also, it was shown that the mean Nusselt number could be maximized and the entropy generation minimized by carefully controlling the geometry parameters of the two wavy surfaces.

It may be mentioned here that, several researchers like Karami et al. [17], Tahereh et al. [18] and Goel et al. [19] focused mainly on first-law efficiency of the nanofluid based direct absorption solar collector without

considering entropy generation. Parvin et al. [20], Parvin and Alim [21] incorporated entropy production and irreversibility issue in analyzing the performance as functions of solar irradiance and mass flow rate.

Recently, Kumar et al. [22] reported that gold nanoparticles (Au-NPs) seeded plasmonic nanofluids (PNFs) have shown promising results in overall performance enhancement of direct absorption solar collector (DASC) due to localized surface plasmon resonance (LSPR) effect. On the other hand, to achieve high-efficiency photo-thermal conversion Guo et al. [23] introduced optical fiber as interior light source in a DASC to boost photo-thermal conversion performance of MWCNT-H₂O nanofluids. Authors reported an accomplishment of 64.5% photo-conversion efficiency for 0.010 wt% MWCNT and the optical fiber location of 15 mm.

Based on the above literature, it can be concluded that though entropy generation has been considered by few researchers in evaluating nanofluid-based DASC collector efficiency, effect of physical changes with operating conditions is not focused that much. Hence, there is a need to evaluate the effect of physical diversities and operating conditions on the performance of DASCs. In this regard, an attempt has been made to numerically simulate fluid flow, heat transfer and entropy generation behaviors through a direct-absorption solar collector with the variation of thickness of flow (D) and solid volume fraction (ϕ) of nanoparticles for various nanofluids and water under the solar irradiation value 225W/m² taken from the annual average solar irradiance range in Bangladesh [24]. Results are presented in terms of isotherm distribution, average output temperature, mean Nusselt number, collector efficiency, rate of entropy generation, and Bejan number.

2. Problem formulation

a. Geometric modeling

Fig. 1 shows the geometry of the direct absorption solar collector filled with nanofluid. The fluid is enclosed within the space between the glass cover and the insulated bottom surface of the DASC. Two-dimensional heat transfer analysis is considered for the nanofluid in the DASC with computational domain of surface area, length and height of A, L and D respectively in which direct sunlight is incident on a thin glass cover and the incident solar flux pass through it. The ratios of dimensions of the collector are chosen according to the experimental setup of Verma and Kundan [4]. Four different fluids; Cu-water nanofluid, Al₂O₃-water nanofluid, TiO₂-water nanofluid and water are utilized as the heat transfer medium. The inlet temperature and velocity of the fluid are T_{in} and U_{in} respectively. The bottom wall is insulated, i.e., no heat flux can pass through it. This assumption is based on the case when the bottom surface is highly insulating. In order to model the heat transfer characteristics, the top surface is assumed to be exposed to the ambient atmosphere that loses heat through convection.

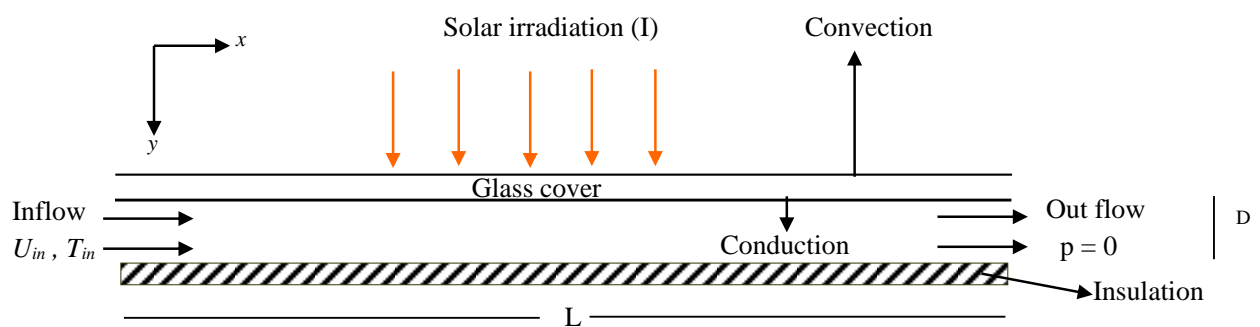


Fig. 1. Geometry of the computational domain of the DASC

b. Thermo-physical properties

In the present study, a comparative heat transfer performance analysis of a DASC system has been performed for base fluid water and, nanofluids Cu-water, Al₂O₃-water and TiO₂. Table 1 gives the thermo-physical properties of water and the nanoparticles [25].

Table 1: Thermo physical properties of fluid and nanoparticles at 300K

Physical Properties	Fluid phase (Water)	Cu Copper	Al ₂ O ₃ Alumina	TiO ₂ Titania
C_p (J/kgK)	4179	385	765	686.2
ρ (kg/m ³)	997.1	8933	3970	4250
k (W/mK)	0.613	400	40	8.9538
β (1/K)	21×10^{-5}	5.1×10^{-5}	2.4×10^{-5}	2.4×10^{-5}

c. *Mathematical modeling*

The nanofluid flow is assumed to be laminar and incompressible. Water and nanoparticles are taken in thermal equilibrium and no slip occurs between them. Boussinesq approximation is used for the density variation of the nanofluid. Only steady state case is considered. The governing equations for the flow throughout a direct absorption solar collector in terms of the Navier-Stokes and energy equations are given as:

Continuity equation:

$$\frac{\partial u}{\partial x} + \frac{\partial v}{\partial y} = 0 \tag{1}$$

x-momentum equation:

$$\rho_{nf} \left(u \frac{\partial u}{\partial x} + v \frac{\partial u}{\partial y} \right) = -\frac{\partial p}{\partial x} + \mu_{nf} \left(\frac{\partial^2 u}{\partial x^2} + \frac{\partial^2 u}{\partial y^2} \right) \tag{2}$$

y-momentum equation:

$$\rho_{nf} \left(u \frac{\partial v}{\partial x} + v \frac{\partial v}{\partial y} \right) = -\frac{\partial p}{\partial y} + \mu_{nf} \left(\frac{\partial^2 v}{\partial x^2} + \frac{\partial^2 v}{\partial y^2} \right) \tag{3}$$

Energy equation:

$$u \frac{\partial T}{\partial x} + v \frac{\partial T}{\partial y} = \alpha_{nf} \left(\frac{\partial^2 T}{\partial x^2} + \frac{\partial^2 T}{\partial y^2} \right) - \left(\frac{1}{\rho C_p} \right)_{nf} \frac{\partial q_r}{\partial y} \tag{4}$$

The energy equation is coupled to the Radiative Transport Equation (RTE)[5] through the divergence of the radiative flux $\frac{\partial q_r}{\partial y} = \int_{\lambda} K_{e\lambda} \tau I_{\lambda} d\lambda$.

Also, $\rho_{nf} = (1 - \phi) \rho_f + \phi \rho_s$ is the density,

$(\rho C_p)_{nf} = (1 - \phi) (\rho C_p)_f + \phi (\rho C_p)_s$ is the heat capacitance,

$\alpha_{nf} = k_{nf} / (\rho C_p)_{nf}$ is the thermal diffusivity,

In the current study, the viscosity of the nanofluid is considered by the Pak and Cho correlation [26]. This correlation is given as

$$\mu_{nf} = \mu_f (1 + 39.11\phi + 533.9\phi^2) \quad (5)$$

and the thermal conductivity of Maxwell Garnett (MG) model [27] is

$$k_{nf} = k_f \frac{k_s + 2k_f - 2\phi(k_f - k_s)}{k_s + 2k_f + \phi(k_f - k_s)} \quad (6)$$

The boundary conditions are:

at all solid boundaries: $u = v = 0$

at the top surface: inward heat flux per unit area $k_{nf} \frac{\partial T}{\partial Y} = q = h_{conv} (T_{col} - T_{amb})$

at the left inlet: $T = T_{in}$ $u = U_{in}$

at the outlet boundary: convective boundary condition $p = 0$

at the bottom surface: $\frac{\partial T}{\partial y} = 0$

d. Average Nusselt number

The average Nusselt number (Nu) is expected to depend on several factors such as thermal conductivity, heat capacitance, viscosity, flow structure of nanofluids, volume fraction, dimensions and fractal distributions of nanoparticles. The form of local heat transfer rate at the top surface is:

$$\overline{Nu} = -\frac{k_{nf}}{k_f} \frac{\partial T}{\partial y} \quad (7)$$

By integrating the local Nusselt number over the top heated surface, the average heat transfer rate along the top surface of the collector can be written as:

$$Nu = \int_0^L \overline{Nu} \, dx \quad (8)$$

e. Entropy generation

The average entropy generation, S for the entire computational domain is as follows:

$$S = \frac{1}{V} \int S_{gen} \, d\bar{V} = S_{gen,h,m} + S_{gen,v,m} \quad (9)$$

where \bar{V} is the volume occupied by the nanofluid and $S_{gen,h,m}$ and $S_{gen,v,m}$ are the average entropy generation for heat transfer and viscous effect respectively [5].

The Bejan number Be , defined as the ratio between the entropy generation due to heat transfer by the total entropy generation, is expressed as:

$$Be = \frac{S_{gen,h,m}}{S} \quad (10)$$

It is known that the heat transfer irreversibility is dominant when Be approaches to 1. When Be becomes much smaller than 1/2 the irreversibility due to the viscous effects dominates the processes and if $Be = 1/2$ the entropy generation due to the viscous effects and the heat transfer effects are equal [14].

f. Collector efficiency

A measure of a collector performance is the collector efficiency (η) defined as the ratio of the useful energy gain to the incident solar energy which can be written as:

$$\eta = \frac{\text{useful gain}}{\text{available energy}} = \frac{mC_p(T_{out} - T_{in})}{AI} \quad (11)$$

where m is the mass flow rate of the fluid flowing through the collector; C_p is the specific heat at constant pressure and T_{in} and T_{out} are the inlet and outlet fluid temperatures, respectively.

3. Methodology

Penalty finite element method (FEM) [28] is used to solve the nonlinear governing equations along with boundary conditions for the considered problem. Due to mass conservation the continuity equation of has been used as a constraint to find the pressure distribution. Eqs. (1) - (4) are solved by the finite element method, where the pressure p is eliminated by a constraint. For large values of this constraint, the equation of continuity is automatically satisfied. Then the velocity components (u, v) and temperature (T) are expanded by means of a basis set. The Galerkin's finite element technique yields the subsequent nonlinear residual equations. The integrals in these equations are evaluated employing three points Gaussian quadrature method. The non-linear residual equations are solved using Newton–Raphson method to determine the coefficients of the expansions. The convergence of solutions is assumed once the relative error for every variable between successive iterations is recorded below the convergence criterion $|\psi^{n+1} - \psi^n| \leq 10^{-4}$, where n is the number of iteration and ψ is any function of u, v and T .

a. Discretization

In the FEM, mesh generation is the procedure to subdivide a domain into a set of sub-domains, named finite elements, control volume, etc. The discrete locations are defined by the numerical grid, at which the variables are to be calculated. It is principally a discrete representation of the computational domain on which the problem is to be solved. Fig. 2 displays the finite element mesh of the present physical domain. Physics controlled mesh is created for the model where free triangular element with unstructured grid is used for discretization.



Fig. 2. Discretization of the computational domain

b. *Grid independent test*

A wide-ranging mesh testing process is carried out to guarantee a grid-independent solution at $I = 225 \text{ W/m}^2$, $m = 0.15 \text{ kg/s}$, $D = 0.015 \text{ m}$ and $\phi = 2\%$ in a DASC. In the present work, five different non-uniform grid systems with the following number of elements within the resolution field: 48, 192, 768, 1616 and 3072 are examined. The numerical method is performed for the values of average Nusselt number for water-Cu nanofluid as well as base for the abovementioned elements to develop a perceptible of the grid fineness as shown in Table 2 and Fig. 3. The scale of the average Nusselt numbers for nanofluid and base fluid for 1616 elements shows a little difference with the results obtained for the more elements. Hence, the non-uniform grid system of 1616 elements are chosen for the whole numerical computation.

Table 2: Grid sensitivity test at $I = 225 \text{ W/m}^2$, $m = 0.15 \text{ kg/s}$, $D = 0.015 \text{ m}$ and $\phi = 2\%$

Nodes (elements)	407 (48)	1434 (192)	5360 (768)	9484 (1616)	20700 (3072)
Nu(nanofluid)	2.40051	2.89143	3.30279	3.582503	3.609242
Nu(base fluid)	1.30253	1.61958	1.93253	2.13084	2.15753
Time (s)	126.265	312.594	398.157	481.328	929.377

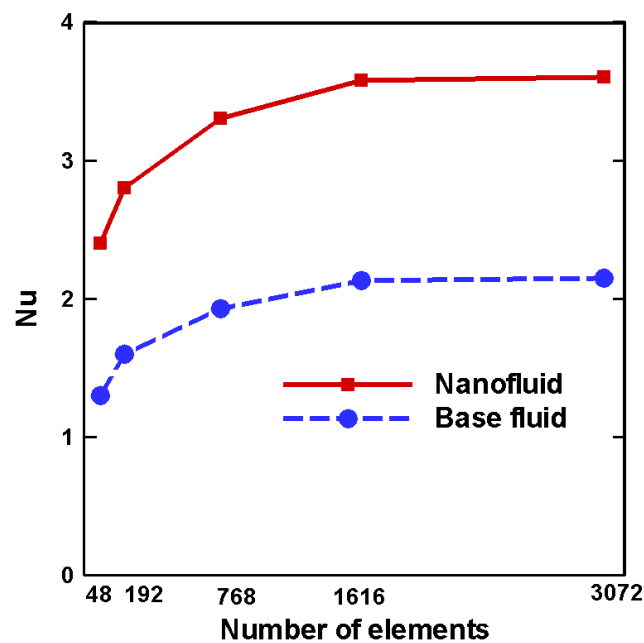


Fig. 3. Grid independence analysis

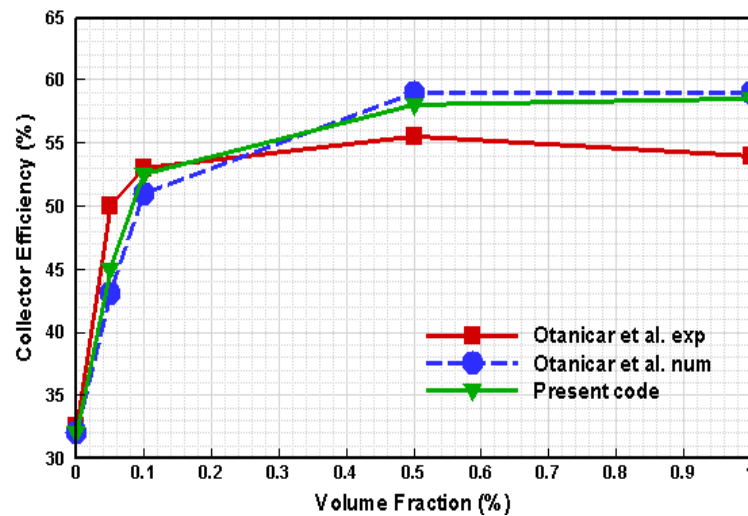


Fig. 4. Comparison of collector efficiency between present code and Otanicar et al. [7] at $I = 1000 \text{ W/m}^2$

c. Validation

The present numerical procedure is validated with the graphical representation of Otanicar et al. [7] for collector efficiency (%) versus volume fraction (%) of water/graphite nanofluid of 30 nm spherical graphite nanoparticles. The validation was carried out in a direct absorption solar thermal collector at irradiation level $I = 1000 \text{ W/m}^2$ and mass flow rate = 42 ml/h, respectively, which are used in [7] for modelling and experiment. Fig. 4 exhibits very good agreement of the numerical results obtained in present work with those reported by Otanicar et al. [7] for the above stated condition.

4. Results and Discussion

Numerical simulation has been carried out to display the outcomes in terms of isotherms, average temperatures at the outlet, average Nusselt number, percentage of collector efficiency, mean entropy generation and Bejan number for different values of parameters flow thickness and solid volume fraction for a DASC filled with various nanofluids. The considered values of flow thickness are $D = 0.012, 0.015, 0.018, 0.02 \text{ m}$ and solid volume fraction are $\phi = 0\%, 1\%, 2\%, 3\%$ and 4% . Three different nanofluids; Cu-water, Al_2O_3 -water and TiO_2 -water are used in addition to the base fluid water. Irradiation $I = 225 \text{ W/m}^2$ and mass flow rate $m = 0.015 \text{ kg/s}$ are found to be most effective in transferring heat and have been chosen for this simulation.

a. Effect of solid volume fraction

Fig. 5 (a) - (d) stands for the effect of solid volume fraction ϕ on the thermal fields. The values of ϕ varies from 0% to 3%. Isotherms are almost like the active parts for water-copper nanofluid. The temperature distributions show that due to escalating values of ϕ , the maximum temperature in the domain rises which results an enhancement in the overall heat transfer. This effect can be accredited to the dominance of the thermal conductivity property. It is worth noting that as the values of ϕ increase, the rate of increment is notable up to the solid volume fraction 2%.

The average outlet temperature, average Nusselt number and collector efficiency for various ϕ are exhibited in Fig. 6 (a)-(c). Different nanofluids and pure water are tested. Parabolic profiles are seen for ϕ versus the average outlet temperature, average heat transfer rate and collector efficiency for all nanofluids. Like profiles are observed in all three figures. Output temperature, heat transfer rate and collector efficiency rise for raising the values of ϕ from 0% to 2% then these values increase at a very slow rate and become

independent of ϕ for $\phi > 3\%$. This occurs due to the fact that for higher concentration of nanoparticles, sedimentation in the fluid starts and movement of the fluid becomes slower which reduces the heat transport process and consequently the efficiency of the collector.

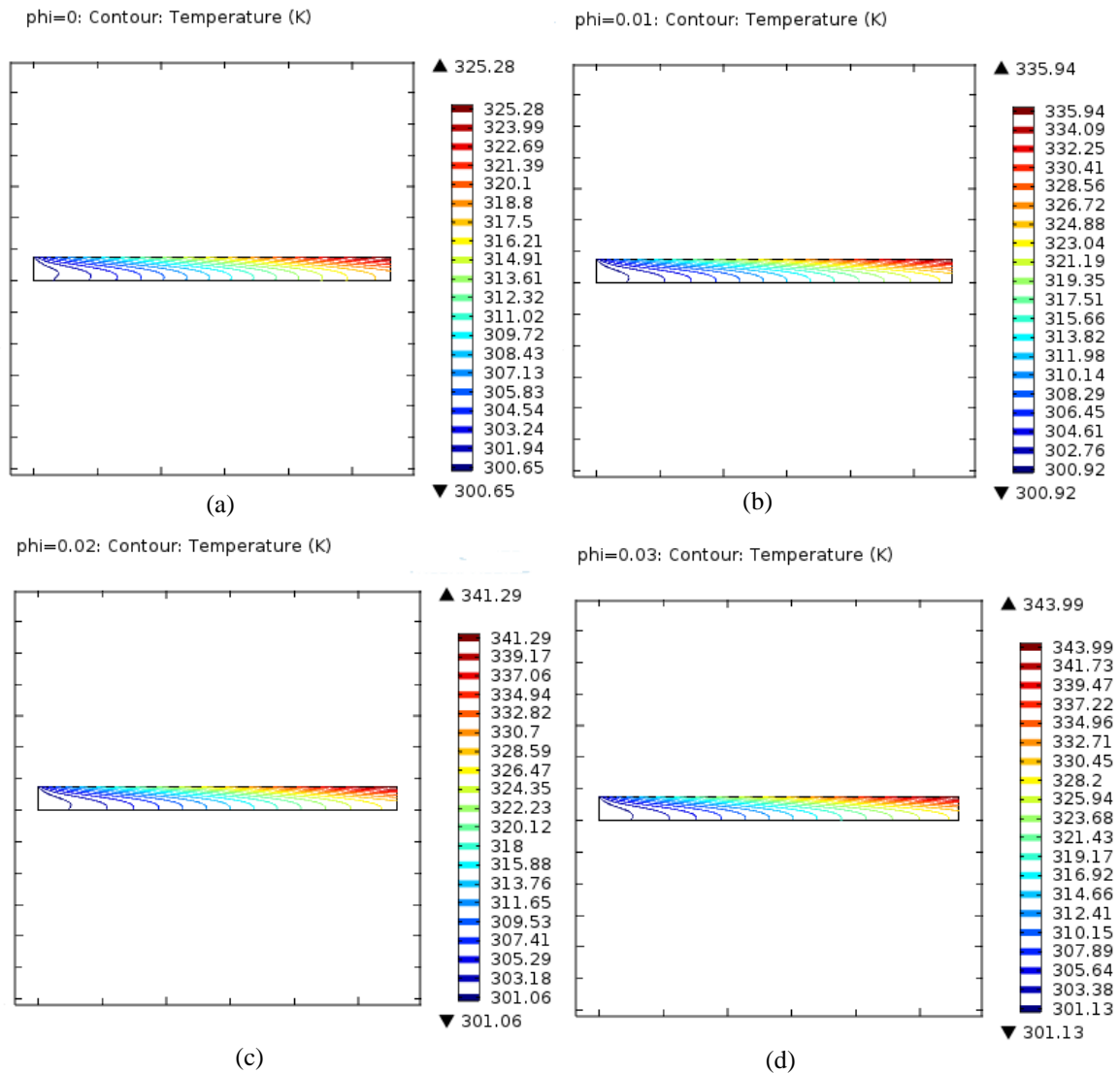


Fig. 5. Isothermal contours for different solid volume fraction (a) $\phi = 0\%$, (b) $\phi = 1\%$, (c) $\phi = 2\%$, and (d) $\phi = 3\%$ with $I = 225$ (W/m^2), $m = 0.015$ (kg/s) and $D = 0.015$ (m) for Cu-water nanofluid.

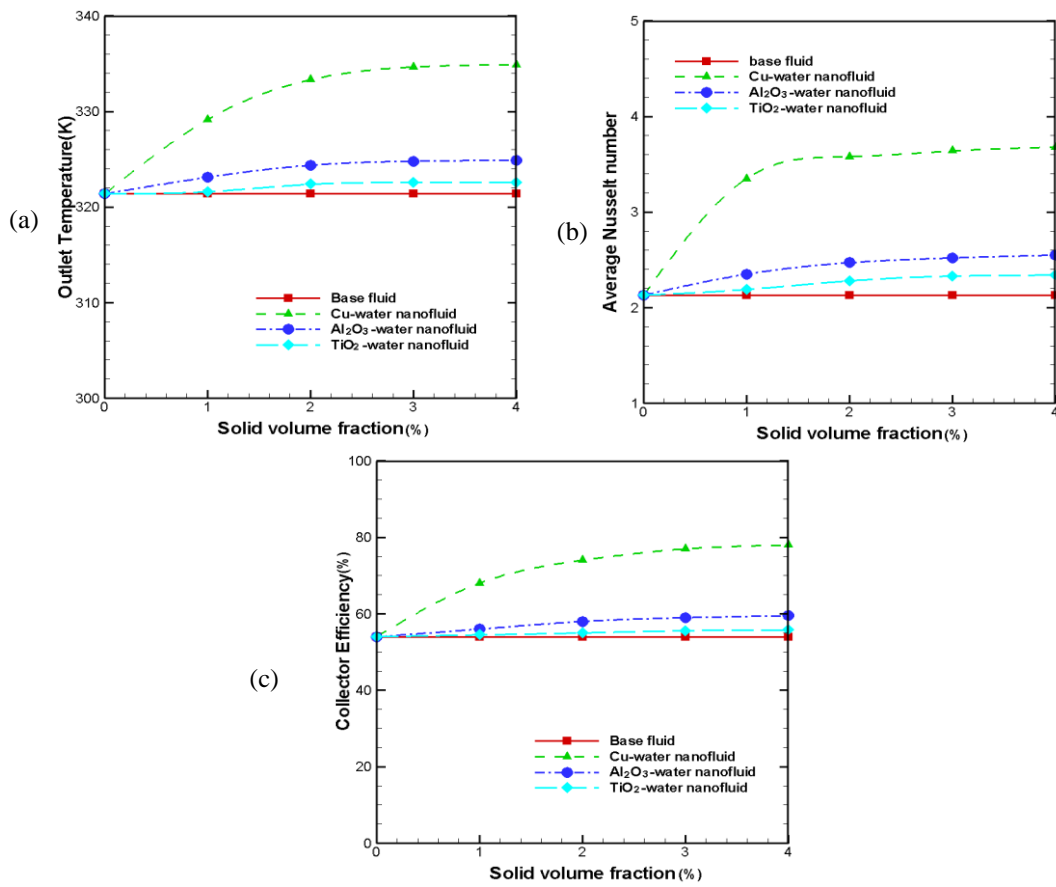


Fig. 6. Effect of solid volume fraction on (a) average output temperature, (b) Average Nusselt number and (c) collector efficiency with $I = 225 \text{ (W/m}^2\text{)}$, $m = 0.015 \text{ (kg/s)}$ and $D = 0.015\text{(m)}$ for different nanofluid as well as base fluid.

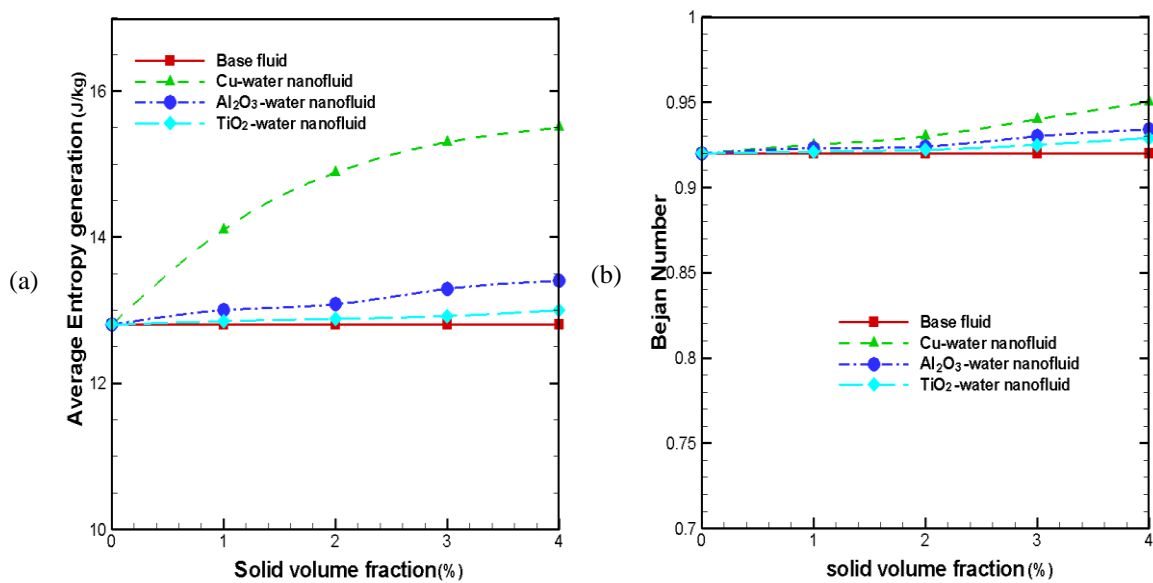


Fig. 7. Effect of solid volume fraction on (a) average entropy generation and (b) Bejan number with $I = 225 \text{ (W/m}^2\text{)}$, $m = 0.015 \text{ (kg/s)}$ and $D = 0.015\text{(m)}$ for different nanofluid as well as base fluid.

Fig 7 (a)-(b) depicts the effects of nanoparticle concentration on entropy generation and Bejan number for various nanofluid and base fluid. The entropy generation rises as the nanoparticle concentration rises. Entropy production has the similar effect as the heat transfer for growing values of solid volume fraction. From the Bejan number versus ϕ picture, it is clearly seen that entropy generation occurs due to the dominant heat transfer effect and this effect becomes larger corresponding to upper ϕ values.

b. Effect of flow thickness

The influence of depth of fluid in a DASC for four different values; $D = (0.012, 0.015, 0.018, 0.02)$ [m] on isothermal contours are exposed in Fig. 8 (a)-(d). From the figure, it is observed that larger flow thickness cannot always raise the temperature. For the calculated values, flow depth of 0.015 [m] is found to give the maximum temperature. Fluid mass becomes greater with escalating the flow depth. That is larger amount of fluid also collects the same amount of heat and transmits though the larger domain. Thus, maximum temperature falls after a certain depth of flow.

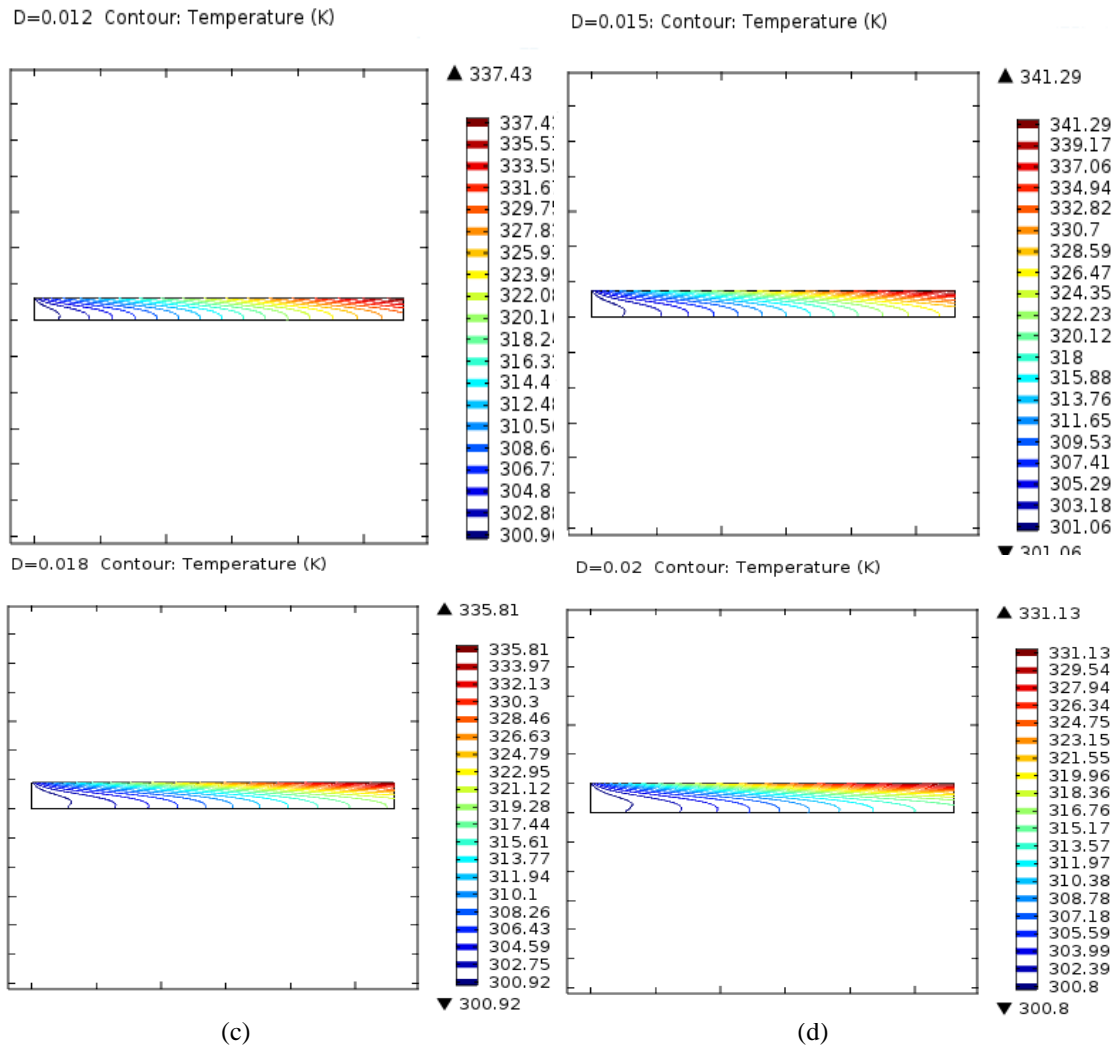


Fig. 8. Isothermal contours for different flow thickness (a) $D = 0.012(m)$, (b) $D = 0.015(m)$, (c) $D = 0.018(m)$, and (d) $D = 0.02(m)$, with $\phi = 2\%$, $m = 0.015$ (kg/s) and $I = 225$ (W/m^2) for Cu-water nanofluid.

Fig. 9 (a)-(c) demonstrates how the distance between the upper and lower surface affects the average

temperature of the outlet, average heat transfer rate and collector efficiency for various nanofluid and base fluid. The 2% concentration is preferred for the nanofluids. The average outlet temperature, average heat transfer rate and collector efficiency for all nanofluid and base fluid slightly increase as the value of D increase from 0.012[m] to 0.015[m] and after that they devalues monotonically with deeper flow. The reason behind this is the deeper flow correspond to larger fluid mass cannot transport more amount of heat from the upper surface. Therefore, collector efficiency cannot be enhanced by choosing greater flow thickness. Similar phenomena are observed for all the considered fluids. However, the Cu-water nanofluid is found to be most effective in enhancing the performance of the collector.

The effects of flow thickness on entropy generation and Bejan number for various nanofluid and water are plotted in Fig 10 (a)-(b). The entropy generation rises by the deepness of the flow. The enhancement of entropy production becomes slower for higher depth of flow. Although the heat transfer reduces for higher collector depth, but entropy production grows because viscosity plays a part here in escalation the entropy generation which is also explained from the Bejan number profile. The Bejan number profile shows the falling trend with larger flow depth. The entropy generation because of viscous term increasing but still heat transfer entropy is leading since the values of Bejan number is much higher than 0.5.

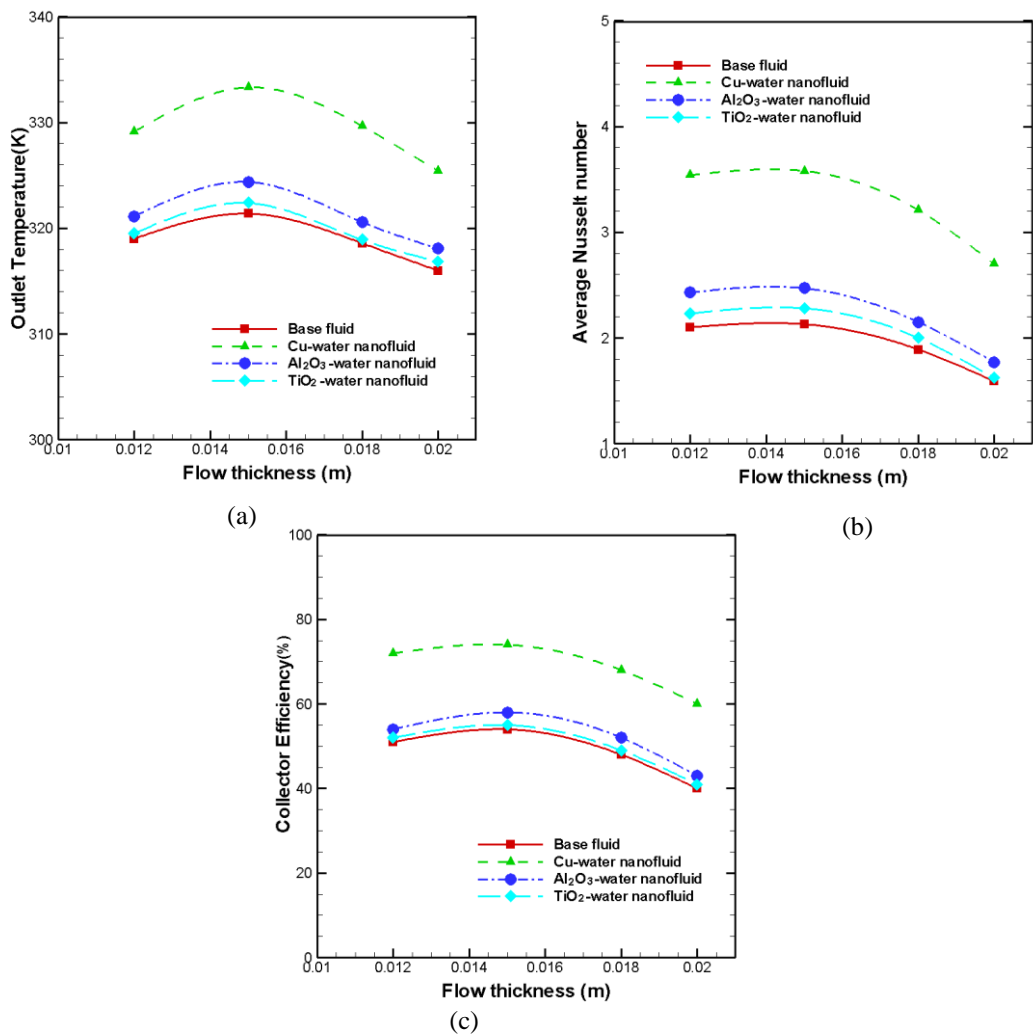


Fig. 9: Effect of flow thickness on (a) average output temperature, (b) Average Nusselt number and (c) collector efficiency with $\phi =$

2%, $I = 225$ (W/m^2) and $m = 0.015$ (kg/s) for different nanofluid as well as base fluid.

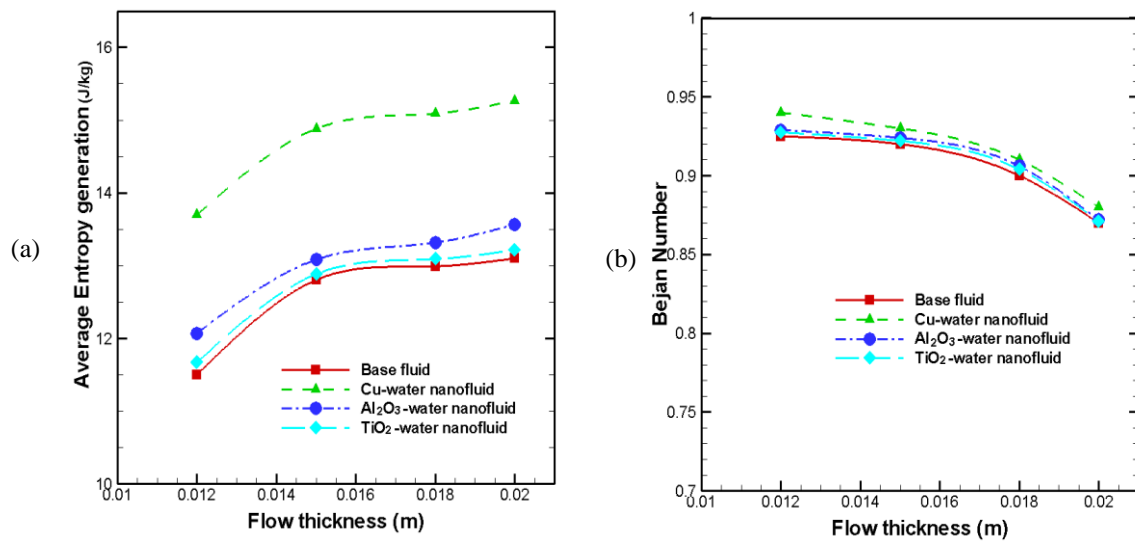


Fig. 10: Effect of flow thickness on (a) average entropy generation and (b) Bejan number with $\phi = 2\%$, $I = 225$ (W/m^2) and $m = 0.015$ (kg/s) for different nanofluidas well as base fluid.

5. Conclusions

In the present article, heat transfer performance of a nanofluid based DASC system has been investigated considering entropy generation under diverse physical orientations and operating conditions. Effect of different combinations of parameters has been examined to observe the output temperature variation. Besides, heat transfer rate, collector efficiency, average entropy generation and Bejan number of the working fluids have been evaluated.

The following inferences are drawn from the present research:

- The isotherms inside the solar collector are remarkably influenced by nanoparticle concentration and depth of flow.
- Rate of heat transfer and efficiency enhances significantly for raising the fluid layer height up to 0.015m. Further increase in fluid layer will lower the average Nusselt number and collector efficiency.
- Higher heat transport and efficiency are observed for nanofluids than the base fluid. Cu- water gives superior efficiency than Al₂O₃- water and TiO₂- water nanofluid.
- Mean entropy generation is obtained higher for rising values of all parameters.
- Bejan number approaches to 1 for the variation of all the parameters. That is the entropy production occurs mainly due to the heat transfer irreversibility though for higher flow thickness, the fluid friction irreversibility tends to rise.

- The nanofluid containing 2% Cu nanoparticles with combination of the solar irradiation 225W/m^2 , mass flow rate 0.015 kg/s and flow thickness 0.015m are established to be most effective in enhancing heat transfer rate and collector efficiency.

It is concluded that higher efficiency of the collector can be obtained by making proper combination of parameters in order to minimize the entropy generation and enhance the heat transfer rate simultaneously.

Nomenclature	
A	surface area of the collector (m^2)
Be	Bejan number
C_p	specific heat at constant pressure ($\text{J kg}^{-1} \text{K}^{-1}$)
D	depth of the fluid (m)
h	local heat transfer coefficient ($\text{Wm}^{-2}\text{K}^{-1}$)
I	intensity of solar radiation (Wm^{-2})
k	thermal conductivity ($\text{W m}^{-1}\text{K}^{-1}$)
L	length of the collector (m)
m	mass flow rate (kgs^{-1})
Nu	Nusselt number
q	heat flux (Wm^{-2})
q_r	radiative heat flux (Wm^{-2})
T	temperature (K)
u, v	x and y components of velocity (ms^{-1})
U	fluid velocity (ms^{-1})
x, y	dimensional co-ordinates (m)
Greek symbols	
α	fluid thermal diffusivity (m^2s^{-1})
ϕ	nanoparticles volume fraction
η	collector efficiency (%)
ρ	density (kgm^{-3})
μ	dynamic viscosity ($\text{kgm}^{-1}\text{s}^{-1}$)
Subscripts	
f	fluid
nf	nanofluid
in	input
out	output
s	solid particle

Conflict of Interests

The authors declare no conflict of interest with any person or agency regarding the content of this article.

Acknowledgements

This research has been conducted in the Department of Mathematics, Bangladesh University of Engineering & Technology (BUET), Dhaka and is supported by the Research Support and Publications Division, UGC, 29/1 Agargaon, Dhaka 1207, Bangladesh.

Funding

Research Support and Publications Division, University Grants Commission (UGC), Bangladesh.

References

- [1] Garg, H.P., Prakash, J, Solar energy fundamental and applications, Tata McGraw Hill, New Delhi(1997).
- [2] Taylor A.R, Phelan E.P, Otanicar P.T, Walker A.C, Nguyen M., Trimble S, Ravi P, Applicability of nanofluids in high flux solar collectors, *International Journal of Renewable and Sustainable Energy*, 3: 023104 (2011).
- [3] Taylor, A.R., Phelan, E.P., Otanicar, P.T, Adrian, R., Prasher, R., Nanofluid optical property characterization: towards efficient direct absorption solar collectors, *Nanoscale Research Letters*, 6: 225 (2011).
- [4] Verma, V., Kundan, L., Thermal performance evaluation of a Direct Absorption Flat Plate Solar Collector (DASC) using Al₂O₃-H₂O based nanofluids, *IOSR Journal of Mechanical and Civil Engineering*, 6 (2): 29-35, (2013).
- [5] Parvin, S., Nasrin, R., Alim, M.A., Heat transfer and entropy generation through nanofluid filled direct absorption solar collector, *International Journal of Heat and Mass Transfer*, 71: 386–395 (2014).
- [6] Tyagi, H., Phelan, P., Prasher, R., Predicted efficiency of a low-temperature nanofluid-based direct absorption solar collector, *Journal of Solar Energy Engineering*, 131 (4): 041004-041010(2009).
- [7] Otanicar, T.P., Phelan, P.E., Prasher, R.S., Rosengarten, G. and Taylor, R.A., Nanofluid-based direct absorption solar collector, *Journal of Renewable and Sustainable Energy*, 2: 033102 (2010).
- [8] Mahian, O., Kianifar, A., Kalogirou, S.A., Pop, I., Wongwises, S., A review of the applications of nanofluids in solar energy, *International Journal of Heat and Mass Transfer*, 57: 582–594 (2013).
- [9] Alsabery, A.I.; Parvin, S.; Ghalambaz, M.; Chamkha, A.J.; Hashim, I. Convection Heat Transfer in 3D Wavy Direct Absorber Solar Collector Based on Two-Phase Nanofluid Approach. *Applied Science*, 10: 7265 (2020).
- [10] Bejan A. A study of entropy generation in fundamental convective heat transfer. *Journal of Heat Transfer-Transactions of the ASME*, 101: 718-725 (1979).
- [11] Bejan A. Entropy generation minimization: the method of thermodynamic optimization of finite-size systems and finite-time processes. Boca Raton: CRC Press, Florida, USA (1996).
- [12] Khorasanizadeh H, Nikfar M, Amani J. Entropy generation of Cu–water nanofluid mixed convection in a cavity. *European Journal Mechanics B-Fluid*, 37: 143–152 (2013).
- [13] Mohseni-Languri, E., Taherian, H., Masoodi, R. and Reisel, J.R. An energy and exergy study of a solarthermal air collector, *Thermal Sciences*, 13(1): 205-216 (2009).
- [14] Shahi M, Mahmoudi AH, Raouf AH. Entropy generation due to natural convection cooling of a nanofluid. *International Communications in Heat and Mass Transfer*, 38: 972-983 (2011).

- [15] Esmailpour M, Abdollahzadeh M. Free convection and entropy generation of nanofluid inside an enclosure with different patterns of vertical wavy walls. *International Journal of Thermal Sciences*, 52: 127-136 (2012).
- [16] Cho CC, Chen CL, Chen CK. Natural convection heat transfer and entropy generation in wavy-wall enclosure containing water-based nanofluid. *International Journal of Heat and Mass Transfer*, 61: 749-758 (2012).
- [17] Karami, M., Akhavan-Bahabadi, M.A., Delfani, S., Raisee, M., Experimental investigation of CuO nanofluid-based Direct Absorption Solar Collector for residential applications, *Renewable and Sustainable Energy Reviews*, 52: 793–801 (2015).
- [18] Tahereh B. Gorji, A.A. Ranjbar, A review on optical properties and application of nanofluids in direct absorption solar collectors (DASCs), *Renewable and Sustainable Energy Reviews*, 72(C):10-32 (2017).
- [19] Goel N., Taylor R.A., Otanicar T., A review of nanofluid-based direct absorption solar collectors: Design considerations and experiments with hybrid PV/Thermal and direct steam generation collectors, *Renewable Energy*, 145: 903-913, 2020.
- [20] Parvin S., Ahmed M. S., Chowdhury R., Effect of Solar Irradiation and Mass Flow Rate on Forced Convective Heat Transfer through a Nanofluid-Based Direct Absorption Solar Collector, *AIP Conference Proceedings* 1851: 020067 (2017). doi: 10.1063/1.4984696.
- [21] Parvin S., and Alim M.A., Influence of Mass Flow Rate on Forced Convective Heat Transfer through a Nanofluid Filled Direct Absorption Solar Collector, *International Journal of Mechanical and Mechatronics Engineering*, 11(6)(2017).
- [22] Kumar, Sanjay & Sharma, Vipin & Samantaray, Manas R. & Chander, Nikhil, Experimental investigation of a direct absorption solar collector using ultra stable gold plasmonic nanofluid under real outdoor conditions, *Renewable Energy*, 162(C): 1958-1969 (2020).
- [23] Guo, C., Liu, C., Jiao, S., Wang, R., Rao, Z., Introducing optical fiber as internal light source into direct absorption solar collector for enhancing photo-thermal conversion performance of MWCNT-H₂O nanofluids. *Applied Thermal Engineering*, 173: 115207 (2020).
- [24] David Mengen & Firoz Aaron, Solar Irradiance Measuring sites in Bangladesh, SrepGen Projects Report of UNDP (2018).
- [25] Ogut, E.B., Natural convection of water-based nanofluids in an inclined enclosure with a heat source, *Int. J. of Thermal Sciences*, 48(11): 2063-2073 (2009).
- [26] Pak, B.C., Cho, Y., Hydrodynamic and heat transfer study of dispersed fluids with submicron metallic oxide particle, *Experimental Heat Transfer*, 11: 151-170 (1998).
- [27] Maxwell-Garnett, J.C., Colours in metal glasses and in metallic films. *Philos. Trans. Roy. Soc. A* 203, 385-420, 1904.
- [28] Reddy, J.N. and Gartling, D.K., *The Finite Element Method in Heat Transfer and Fluid Dynamics*, CRC Press, Inc., Boca Raton, Florida, USA (1994).